J. theor. Biol. (1978) **72**, 161–184

Hepatic Elimination of Flowing Substrates: The Distributed Model

L. BASS, P. ROBINSON AND A. J. BRACKEN

Department of Mathematics, University of Queensland, St. Lucia, Brisbane, Australia

(*Received* 18 *April* 1977, *and in revised form* 8 *November* 1977)

An earlier model of hepatic elimination with functionally identical sinusoids is extended by introducing statistical distributions of enzyme contents per sinusoid and of blood flow per sinusoid, these being either uncorrelated or closely correlated. The steady-state theory of the resulting distributed model is developed, including methods of determining experimentally the coefficients of variation of the distributions. Such determinations are made on an illustrative experimental example. Quantitative predictions of expected effects of changes in blood flow are given, including one for which the undistributed model predicts a null effect. Shapes of the postulated distributions are discussed only in relation to observable effects. Effects of the distributions are compared with maximum possible effects of incomplete equilibration of substrate within each sinusoidal cross-section, and methods for distinguishing these effects from each other are outlined.

1. Introduction

When hepatic enzymes eliminate substrates dissolved in the blood, the liver acts as a set of many similar and independent elements arranged in parallel. Each element consists of an anatomically defined passage (called *sinusoid*) perfused with blood carrying the substrates, and lined with liver cells (*hepatocytes*) containing the enzymes.

An experimentally supported model of such elimination has been developed (Bass, Keiding, Winkler & Tygstrup, 1976, denoted BKWT in what follows) for a class of substrates (such as galactose or ethanol) which are eliminated in each liver cell by a Michaelis–Menten process, without the overall elimination rate of the intact liver being limited by any diffusion step. In that model each element has a maximum elimination rate v_{max} observed at saturation; the latter is controlled by the Michaelis constant K (we shorten the more usual notation K_m). Unidirectional blood flow through the element will be denoted by f. The relation between the

0022–5193/78/0508–0161 $02.00/0

substrate concentration c_i at the inlet (influx fc_i) and c_o at the outlet (outflux fc_o) which characterizes steady-state elimination, is determined in each element entirely by the two quantities v_{max}/f and K:

$$c_i - c_o + K \ln (c_i/c_o) = v_{max}/f. \quad (1)$$

The steady elimination rate v in each element is given by the difference between the influx and the outflux of substrate:

$$v = f(c_i - c_o). \quad (2)$$

Liver anatomy ensures that c_i is common to all elements. Outfluxes from all elements are mixed well before they can reach a liver vein catheter.

If v_{max}/f and K were the same pair of numbers in each element, the common c_i would result in a common c_o. On this assumption, simple addition of elements in parallel gives an approximate picture of steady-state liver elimination [BKWT] which we shall call the *undistributed* model. Observations support that assumption to the extent that coefficients of variation of v_{max}/f and of K for elements constituting an actual human or pig liver may be expected to be small [BKWT especially Appendix A].

The Michaelis constant K is a specific chemical constant relating to each molecular enzyme-substrate interaction, and is therefore likely to be identical in each element (see also section 4). By contrast, v_{max} and f are additive macroscopic quantities determined in each element by the number and configuration of its constituent cells, in a manner which is unlikely to render v_{max} and f exactly proportional to each other. In the present paper we therefore assume that v_{max}, f and v_{max}/f may be distributed over the elements constituting each liver. From the earlier work [BKWT] we adopt the steady-state theory of the *single* element based on equations (1) and (2), and the conclusion that the distributions are narrow in a sense specified below. On these assumptions we develop the *distributed* model of steady elimination, we deduce observable consequences permitting the estimation of the widths of the distributions, and make these estimates for actual experimental examples used earlier [BKWT]. We also make quantitative predictions of the effects of changes in blood flow, and in particular present one effect in a form for which the undistributed model predicts a null effect.

In some actual livers, especially in cirrhosis, there probably exist passages for blood flow which are in parallel to the normal elements but not lined with hepatocytes containing enzymes. Such passages are known as intrahepatic shunts (Prinzmetal *et al.*, 1948; Popper, Elias & Petty, 1952) and are harmful because they permit free passage of toxic substances from the intestines. If these shunts were included in the distributed model as a subset of elements with v_{max} close to zero, then the set of all elements would have a

two-peaked distribution of v_{max}-values with a large coefficient of overall variation, contrary to our assumption. We show briefly in section 4 how effects of shunts, where they exist, can be determined and subtracted out, leaving an effective shunt-free liver satisfying the assumptions of the distributed model. A systematic experimental study of the distributed model will be given elsewhere, with emphasis on the detection and determination of intrahepatic shunts and on clinical interpretations of the distributions.

The number of elements represents the fineness of the division of blood flow through the liver. The blood volume of a human or pig liver is of the order of 250 cm^3, the length of sinusoids in the flow direction is about 0·1 cm and their smallest width is about 10^{-3} cm (see Winkler *et al.*, 1974, for these and following estimates). The number of elements is overestimated if we assume that the greatest width of sinusoids is also 10^{-3} cm, so that the number of elements would be about $250/[(10^{-1})\,(10^{-3})^2] = 2{\cdot}5 \times 10^9$. In reality the sinusoids are more alike to pairs of folded parallel cell plates distant 10^{-3} cm, not as wide as they are long. Thus the number of elements is more than $250/[10^{-1})^2(10^{-3})] = 2{\cdot}5 \times 10^7$. These large numbers ensure the possibility of approximately continuous distributions of properties of the elements. Moreover, the large numbers arise from anatomical magnitudes that have important functional aspects. The evident requirement of the free passage of blood cells through the liver is satisfied by the smallest width of the sinusoids. On the other hand, the transverse diffusion time of substrates in the sinusoids is as short as is consistent with the free passage of blood cells: for typical substrate diffusion coefficients of the order 10^{-5} $cm^2\ s^{-1}$, the transverse diffusion time is about $(10^{-3})^2/10^{-5} = 10^{-1}$ s, which is about a hundred times shorter than the shortest time of transit of fluid elements through the liver (Goresky, Bach & Nadeau, 1973). This time factor ensures that substrates do not readily escape the influence of enzymes at the walls, whereby an intrahepatic shunt would be simulated. In reality, the transverse equilibration time is reduced by convective mixing in bolus flow (Prothero & Burton, 1961), appreciably so for substrates with diffusion coefficients smaller than those of ethanol and galactose, i.e. for Peclet numbers appreciably above unity in each bolus (Aroesty & Gross, 1970). Hence 10^{-1} s must be regarded as an upper limit for the transverse equilibration time. The corresponding maximum possible effects of incomplete transversal equilibration of arbitrary substrates will be discussed further in Appendix C.

We develop the distributed model for two anatomically distinct cases:

(i) v_{max} and f are each distributed narrowly, and the two distributions are independent (uncorrelated). This case may be envisaged as the perturbation

of the undistributed liver by small random deviations in the construction of the elements.

(ii) v_{max} and f may each be distributed widely, but they are nearly proportional: v_{max}/f is distributed narrowly. Moreover, the distribution of v_{max}/f is independent of (uncorrelated with) the distribution of f. This case may be realized approximately in local necrosis, where failing blood supply reduces the number of enzymatically active hepatocytes and where, moreover, the resulting proportionality of v_{max} and f is perturbed randomly by the variability of this necrotic process.

The analysis proceeds by successive approximations on the assumption that to successive moments of narrow distribution functions there correspond successively smaller contributions to the values of observable quantities. For clarity of presentation we first develop in section 2 the special case of (i) where v_{max} has a narrow distribution and f is undistributed. This is done by deviating from an initially undistributed liver by envisaging transfers of enzyme between elements, whereby a discrete distribution of v_{max} with some mean $\bar{v}_{max}$ and variance σ^2 is generated. In the lowest order of approximation we find that large transfers between few elements produce the same effects on observable quantities as small transfers between a large number of elements, provided $\bar{v}_{max}$ and σ^2 are the same in each case. Furthermore, the effects are the same as those due to a continuous distribution of v_{max} with the same mean and variance, as we show in Appendix A where the theory is developed in the lowest order of approximation for continuous distributions in both the cases (i) and (ii). Results of higher orders of approximation are discussed in section 3, where we show how symmetric and asymmetric discrete distributions resulting from enzyme transfers generalize the effects of a narrow normal distribution of the same mean and variance. Full higher-order calculations will be given elsewhere (Robinson, Ph.D. Thesis).

While in sections 2 and 4 the principal observable effects are derived by elementary means applied to limiting regimes of elimination, all regimes and all ranges of the relevant parameters are dealt with in the lowest order of approximation in Appendix B. The Discussion (section 4) includes methods of determining the coefficient of variation $\sigma/\bar{v}_{max}$ of a distribution by varying the inflow concentration c_i, illustrated by an experimental example, as well as predictions of the effects of changes in blood flow.

Distributions of sinusoidal flows f must be distinguished from distributions of transit times observed by means of dilution curves of radioactive tracers (Goresky *et al.*, 1973). In the simplest case of convective transport of labelled cells through a sinusoid of volume v, the transit time t is given by $t = v/f$. Now, the sinusoidal volumes are likely to have a distribution of

their own in any one liver. Thus, even the undistributed model of elimination [BKWT] would be consistent with the observed distributions of t if the latter were due entirely to distributions of v (e.g. to distributions of lengths of tubes with identical f-values). In the distributed model, f-distributions would be equal to the distributions of (inverse) t only if the sinusoidal volumes were undistributed. More generally, relations between distributions of t and f are not known because the distributions of v are not known.

2. Discrete Distributions

We consider first a model liver consisting of N elements with v_{max} distributed narrowly about the mean $\bar{v}_{max}$ with variance σ^2 and coefficient of variation $\varepsilon = \sigma/\bar{v}_{max}$; f and K are undistributed. We start from an undistributed liver which has the same values of N and K, the same total hepatic flow F and the same maximum elimination rate V_{max} of the whole liver ($v_{max} = V_{max}/N, f = F/N$), so that the two livers are macroscopically corresponding to each other in that they have the same macroscopic parameters. We envisage transfers of units of enzyme equivalent to δv_{max} each, from a fraction $\alpha/2$ of the N elements to a fraction $\alpha/2$ of other elements, leaving the fraction $1 - \alpha$ of elements unchanged. In this process the mean $\bar{v}_{max}$ remains equal to the v_{max} of the unaffected elements, V_{max} is unchanged, and a symmetric discrete distribution of v_{max} is obtained with

$$\left.\begin{aligned} \sigma^2 &= \overline{(v_{max} - \bar{v}_{max})^2} = \alpha(\delta v_{max})^2 \\ \varepsilon^2 &= \alpha(\delta v_{max}/\bar{v}_{max})^2, \quad 0 \leq \alpha \leq 1. \end{aligned}\right\} \tag{3}$$

The effect of the transfers will be to generate a distribution of outflow concentrations c_o with a mean $\bar{c}_o$ (detected by a liver vein catheter). Because of the non-linear dependence of c_o on v_{max}, $\bar{c}_o$ is different from the outflow concentration belonging to elements with the mean $\bar{v}_{max}$, denoted by $c_o(\bar{v}_{max})$. The latter is the same as the c_o of the corresponding undistributed liver before the transfers. In this section we calculate the observable $\bar{c}_o$ by elementary means in the two limiting regimes [BKWT] of very high and very low inflow concentrations c_i.

(A) THE HOMOGENEOUS REGIME

When c_i is so high that all enzyme molecules are close to saturation by substrate, the overall elimination rate must be independent of blood flow and of any structural arrangements. Since elimination is responsible for the difference between the influx and outflux of substrate for the whole liver, $F(c_i - \bar{c}_o)$ approaches V_{max}, giving the same $\bar{c}_o$ and c_o ($\bar{v}_{max}$) regardless of transfers.

(B) THE CLEARANCE REGIME

At the other extreme of sufficiently low c_i, equations (1) and (2) imply [as shown in BKWT] that the outflow concentration c_o from each element is related to the common c_i by:

$$c_o = c_i \exp(-v_{\max}/fK), \tag{4}$$

which characterizes the clearance regime of elimination. After the transfers,

$$\bar{c}_o = (1-\alpha)c_o(\bar{v}_{\max}) + \tfrac{1}{2}\alpha c_i \exp\left(-\frac{\bar{v}_{\max}+\delta v_{\max}}{fK}\right) + \tfrac{1}{2}\alpha c_i \exp\left(-\frac{\bar{v}_{\max}-\delta v_{\max}}{fK}\right)$$

or, using equation (4) again and re-arranging,

$$\bar{c}_o = c_o(\bar{v}_{\max})\{1+\alpha[\cosh(\delta v_{\max}/fK)-1]\}. \tag{5}$$

Thus for any finite $\delta v_{\max}$ we have $\bar{c}_o > c_o(\bar{v}_{\max})$: transfers always increase $\bar{c}_o$ at given c_i, that is, a distributed liver eliminates at a lower rate than an undistributed liver with the same macroscopic parameters. This is because deviations from equal division of substrate amongst the available enzyme molecules reduce the rate of a Michaelis–Menten process. This was shown [BKWT] for unequal divisions *along* sinusoids, but it holds equally for inequalities of division *amongst* elements with common c_i.

For transfers which are small in the sense:

$$\delta v_{\max} \ll fK, \tag{6}$$

we expand equation (5) using the series $\cosh X = 1 + x^2/2 + x^4/24 + \ldots$. We now retain only the quadratic term $\frac{1}{2}\alpha(\delta v_{\max}/fK)^2$ which is, from equation (3), $\frac{1}{2}\varepsilon^2(\bar{v}_{\max}/fK)^2$:

$$\bar{c}_o = c_o(\bar{v}_{\max})(1+\tfrac{1}{2}r^2\varepsilon^2), \tag{7}$$

where we have set:

$$r = \bar{v}_{\max}/(fK) = V_{\max}/(FK). \tag{8}$$

To this order of accuracy, α and $\delta v_{\max}$ appear only in the combination ε^2 so that it is immaterial whether we envisage many small transfers or few larger ones [consistent with inequality (6)], provided ε^2 is the same in each case. This property does not hold to higher orders of approximation (section 3). For the distributed liver in the clearance regime *B*, $\bar{v}_{\max}$ and $c_o(\bar{v}_{\max})$ are connected by a relation of the form of equation (4), and $c_o(\bar{v}_{\max})$ is connected with the observable $\bar{c}_o$ through equation (7). Re-arranging equation (4) and using equations (7) and (8),

$$r = \ln c_i - \ln c_o(\bar{v}_{\max}) = \ln c_i - \ln \bar{c}_o + \ln(1+\tfrac{1}{2}r^2\varepsilon^2).$$

Expanding the last term and again retaining the quadratic ε^2-term, we obtain:

$$r(1-\tfrac{1}{2}r\varepsilon^2) = \ln c_i - \ln \bar{c}_o, \tag{9}$$

which differs from the limiting clearance equation (4) of the corresponding undistributed liver by the replacement of c_o with $\bar{c}_o$, and of r with $r(1-\frac{1}{2}r\varepsilon^2)$ which we denote by r_B. In macroscopic terms, the latter replacement means that V_{max} is replaced in the clearance regime B by $V^B_{max} = FKr_B$,

$$V^B_{max} = V_{max}[1-\tfrac{1}{2}\varepsilon^2(V_{max}/FK)] < V_{max}. \tag{10}$$

The observable difference between the undistributed and distributed models are brought out most clearly by using the concise formulation of the former given in BKWT: writing equations (1) and (2) for the overall liver quantities F and the total elimination rate V, and eliminating F from the two equations, we find that the Michaelis–Menten relation holds for V and the logarithmic average $\hat{c}$ of the inflow and outflow concentrations: $V = V_{max}\hat{c}/(\hat{c}+K)$, or:

$$1/V = 1/V_{max} + (K/V_{max})(1/\hat{c}), \tag{11}$$

yielding a Lineweaver–Burk (L–B for short) straight line for the plot of the inverse quantities $1/V$, $1/\hat{c}$, with the slope K/V_{max}. According to the above results for the corresponding distributed model, equation (11) holds in the limiting regime A after the transfers if the undistributed outflow concentration c_o is replaced by the mean $\bar{c}_o$: $V = F(c_i - \bar{c}_o)$, and

$$\hat{c} = \frac{c_i - \bar{c}_o}{\ln (c_i/\bar{c}_o)}, \quad c_i > \hat{c} > \bar{c}_o \tag{12}.$$

In the opposite limit of regime B, we have $V = V^B_{max}\hat{c}/K$ from equations (9), (10) and (12), so that $d(1/V)/d(1/\hat{c}) = K/V^B_{max}$. The generalization of equations (9) and (11) valid for all inflow concentrations will be given in Appendices A and B, but the principal effect is now apparent (Fig. 1): equation (11) remains valid at low $1/\hat{c}$ as the equation of the tangent at $1/\hat{c} = 0$ to a curved *L.–B.* plot, which has an asymptote at high $1/\hat{c}$ having the steeper slope K/V^B_{max}. The increase Δs of slope from the initial tangent to the asymptote is thus K/V^B_{max}-K/V_{max}. Using equation (10) and retaining terms of order ε^2,

$$\Delta s = \varepsilon^2/2F. \tag{13}$$

The simplicity of this result contrasts with the more complicated analysis of the intersection of the initial tangent and asymptote (Appendix B). It is remarkable that the result (13) remains valid (in the lowest order of

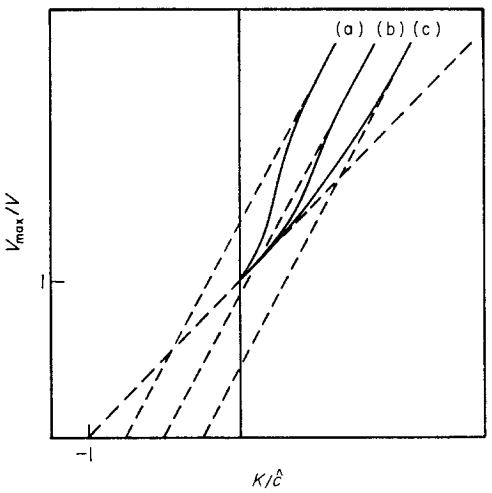

FIG. 1. Inverse elimination rate plotted against inverse logarithmic average of inlet and outlet concentrations of substrate (normalized) for three ranges of $r = V_{max}/FK$. (a) $r > 1{\cdot}25$. (b) $0{\cdot}405 < r < 1{\cdot}25$; the plot intersects its asymptote, in contrast with (a) and (c). (c) $r < 0{\cdot}405$. The distributions are adjusted so that $r\varepsilon^2$ is the same for each curve (the three asymptotes are parallel).

approximation) for each of the cases (i) and (ii) described in the Introduction when continuous distributions are adopted, provided that in case (i) ε^2 is interpreted as the sum of the squares of the coefficients of variation of v_{max} and f, and in case (ii) as the square of the coefficient of variation of v_{max}/f. This we show in Appendix B. Equation (13) furnishes a quantitative and qualitative distinction between the distributed and undistributed models, as well as a means of estimating ε^2 from experiments (section 4).

3. Higher Order Effects

When the series developments of the preceding section are carried to the next higher order in ε, equation (7) becomes:

$$\bar{c}_o = c_o(\bar{v}_{max})[1 + \tfrac{1}{2}r^2\varepsilon^2(1 + r^2\varepsilon^2/12\alpha)]. \tag{14}$$

The additional term is of order ε^4 and increases $\bar{c}_o$ further as compared with $c_o(\bar{v}_{max})$, that is, it reduces elimination further as compared with a corresponding undistributed liver. The additional reduction of elimination at any fixed ε is increased by reducing α, that is, by attaining that ε with fewer (larger) transfers. Thus the influence of α and δv_{max} is no longer confined to the combination $\alpha\delta v_{max}^2$ which determines ε^2 according to equation (3). We note that inequality (6) presupposed by equation (14) ensures that the

additional term remains small: $r^2\varepsilon^2/\alpha$ is the same as $(\delta\, v_{max}/fK)^2$ according to equations (3) and (8).

Extending the calculation of Δs in equation (13) to the next higher order on the basis of equations (14) we obtain:

$$\Delta s = \frac{\varepsilon^2}{2F}\left[1+\tfrac{1}{2}r\varepsilon^2+\tfrac{1}{4}r^2\varepsilon^2\left(\frac{1}{3\alpha}-1\right)\right]. \tag{15}$$

The sign of the last term depends on the value of α, so that the qualitative effect of the ε^4-terms on the slope-change Δs depends, for any given ε, on the values of α and r.

In Appendix A, series developments are made in terms of moments defined for narrow continuous distributions. For normal (Gaussian) distributions, developments to order ε^4 yield equation (14) and equation (15) with $\alpha = 1/3$, so that the last term in equation (15) vanishes. The non-Gaussian character of that last term may be elucidated as follows. The transfer-generated distribution is symmetric about $\bar{v}_{max}$, with odd moments vanishing and the second moment defining ε^2 according to equation (3). The fourth moment is:

$$\overline{(v_{max}-\bar{v}_{max})^4} = \alpha(\delta v_{max})^4 = \sigma^4/\alpha,$$

using equation (3). On the other hand, for a normal distribution the fourth moment is:

$$\frac{1}{\sigma\sqrt{2\pi}}\int_{-\infty}^{+\infty}(v_{max}-\bar{v}_{max})^4 \exp\left[-\frac{1}{2}\left(\frac{v_{max}-\bar{v}_{max}}{\sigma}\right)^2\right] dv_{max} = 3\sigma^4.$$

Only positive values of v_{max} are meaningful: the formal value of the lower integration sign signifies that we are considering distributions which are narrow in the sense $(\bar{v}_{max}/\sigma)^2 = \varepsilon^{-2} \gg 1$ so that the integrand is vanishingly small at $v_{max} \leqq 0$ (see the discussion of shunts in sections 1 and 4). The two fourth moments coincide for $\alpha = 1/3$. Thus transfers lead to more general elimination effects than normal distributions, since in the higher orders the former have the additional degree of freedom α. This is to be preferred, since normal distributions make reference to the meaningless negative values of v_{max} whenever $e^{-1/2\varepsilon^2}$ is not negligibly small compared with unity.

When $\alpha = 1/3$, the ε^4-term in equation (15) always increases the slope-change Δs as compared with equation (13). When some Δs is obtained from experiments (section 4), the ε calculated from equation (15) for a normal distribution ($\alpha = 1/3$) is therefore always smaller than that calculated from the lower approximation in equation (13), the reduction depending on the value of r. An example of such a reduction for pig liver 28/73 is given in section 4.

Normal or, more generally, symmetric narrow distributions are likely in normal livers on probabilistic grounds. In local necrosis (section 1), outright losses of $\delta v_{\max}$ in some fraction of elements are likely, corresponding to loss of enzymatic activity and resulting in asymmetric distributions of $v_{\max}$. Such effects appear in correction terms of order ε^3, as we now outline.

We begin by envisaging a new set of transfers, again starting from a macroscopically corresponding undistributed liver. Let $\delta v_{\max}$ be removed from each of the fraction β of the N elements and distributed equally amongst the remaining $(1-\beta)N$ elements, each of which thus gains $\beta\delta v_{\max}/(1-\beta)$. The mean $\bar{v}_{\max}$ of the resulting distribution remains equal to the $v_{\max}$ of the original elements, while:

$$\left.\begin{aligned} \sigma^2 &= \overline{(v_{\max}-\bar{v}_{\max})^2} = \frac{\beta}{1-\beta}(\delta v_{\max})^2 \\ \varepsilon^2 &= \frac{\beta}{1-\beta}(\delta v_{\max}/\bar{v}_{\max})^2 \end{aligned}\right\}. \tag{16}$$

The resulting distribution may alternatively be interpreted as a necrotic modification of an initially undistributed liver with $v'_{\max} = v_{\max} + \beta\delta v_{\max}/(1-\beta)$ per element, which has lost enzyme equivalent to $\delta v_{\max}/(1-\beta)$ from each of a fraction β of its elements. Calculations analogous to those above, carried to order ε^3, yield:

$$\left.\begin{aligned} \bar{c}_o &= c_o(\bar{v}_{\max})[1+\tfrac{1}{2}r^2\varepsilon^2(1+\tfrac{1}{3}\gamma r\varepsilon)] \\ \gamma &= \frac{1-2\beta}{\sqrt{\beta(1-\beta)}} \end{aligned}\right\}. \tag{17}$$

The ε^2-term is unchanged, as expected. The parameter γ vanishes at $\beta = \frac{1}{2}$ when the distribution is symmetric. At any fixed ε, the ε^3-term increases (reduces) $\bar{c}_o$ further for $\beta < \frac{1}{2}$ ($\beta > \frac{1}{2}$). Carrying the calculation of Δs also to order ε^3, we find

$$\Delta s = \frac{\varepsilon^2}{2F}(1+\tfrac{1}{3}\gamma r\varepsilon), \tag{18}$$

with γ as in equation (17). Again, the sign of the contribution of the ε^3-term to Δs depends on the choice $\beta \lessgtr \frac{1}{2}$.

More detailed consideration of non-Gaussian and non-symmetric distributions will be given elsewhere, with emphasis on their connection with different types of liver damage. In addition to experimental accuracy, the systematic detection of such higher-order terms would require a sufficiently accurate allowance for the diffusional effects outlined in Appendix C.

4. Discussion

The simplest extensions of the undistributed model by equation (7) and (13) arise from the plausible assumption that the relevant properties of the 10^7–10^9 liver elements have a non-zero coefficient of variation ε; their accuracy depends on ε^2 being small. Only in terms involving ε^3 and ε^4 do particular features of the distributions appear. We now return to the observable features of the ε^2-term which is universal in the above sense and which is readily detectable experimentally, as will be shown below.

We note first that the distributed model not only introduces quantities foreign to the undistributed model, but it also modifies the analysis of data determining quantities common to both models, notably K. When V_{max} and K are determined from data plotted on the L–B plot of $1/V$ against $1/\hat{c}$ (Fig. 1), the customary analysis from the slope and intercept of the plot (or its computational equivalent) remains correct only for the initial tangent of the plot (section 2), where the slope of the plot is the least. The statistical fitting of a best straight line to all data-points according to the undistributed model therefore always overestimates K by an amount which increases with ε, and with the degree of clustering of data-points in the intermediate region of $1/\hat{c}$ where the slope goes through a maximum whenever r is greater than $\ln(3/2) \approx 0{\cdot}405$ (Appendix B). It is probably for these reasons that while K is assumed to be undistributed throughout each liver in both the undistributed and distributed models, application of the former to data from a series of isolated perfused pig livers (Keiding *et al.*, 1976, with all values of r exceeding unity) yielded a variation of K's amongst the livers by a factor of 2·5. Such a variation would seem to contradict the common biochemical significance of the observed K's (namely, K_m of the phosphorylation of galactose by galactokinase), but the possibility of a variation in the partition coefficient of the substrate between the blood and the hepatocyte should be remembered [BKWT].

Experiments in which c_i is varied on each liver from the homogeneous regime A to the clearance regime B (section 2) furnish data from which ε^2 can be determined by two separate methods.

(1) The most direct method proceeds without the use of $\bar{c}_o$, but it cannot be used for large values of $r = V_{max}/FK$. We recall from BKWT that when equations (1) and (2) are written for the undistributed liver as a whole (with V and F replacing v and f), elimination of c_o from the two equations yields an L–B-type plot of $1/V$ against $1/c_i$ (Fig. 2). The initial tangent at $1/c_i = 0$ again describes the homogeneous regime A (Michaelis–Menten relation for V and c_i), while the asymptote at high $1/c_i$ describing the clearance

regime B is:

$$1/c_i = F(1-e^{-r})(1/V)-e^{-r}/K. \tag{19}$$

Thus the intercept of the initial tangent with the horizontal axis is $\overline{OB} = 1/K$ and the intercept of the asymptote is $\overline{OA} = e^{-r}/K$ (Fig. 2). Hence the ratio $\overline{OA}/\overline{OB} = e^{-r}$ determines r, which should be equal in the undistributed model to the V_{max}/FK determined from the slope of the initial tangent, K/V_{max}, and from an independent measurement of the hepatic flow F.

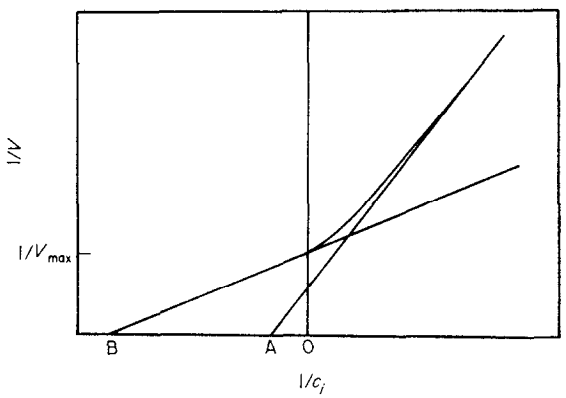

FIG. 2. Inverse elimination rate plotted against inverse inlet concentration of substrate, with asymptote and initial tangent. $\overline{OA}/\overline{OB}$ permits an estimate of the coefficient of variation of the distribution.

Now, the same data determining the same limiting straight lines are used in the distributed model with a modified interpretation: the initial tangent and the the flow determine the correct value of r as before, but $\overline{OA}/\overline{OB}$ must be interpreted as e^{-r_B} with $r_B = V^B_{max}/FK$, where the smaller $V^B_{max} < V_{max}$ is given by equation (10) according to the description of the clearance regime in the distributed model. Thus the slope of the asymptote predicted by the distributed model, $[F(1-e^{-r_B})]^{-1}$, is larger than that given by equation (19) for the macroscopically corresponding undistributed liver. This is because distributions reduce V at any given c_i everywhere outside the homogeneous regime. The knowledge of r and r_B from a plot such as Fig. 2 now permits an estimate of ε^2: inverting equation (10),

$$\varepsilon^2 = 2(r-r_B)/r^2. \tag{20}$$

For example, in pig liver 28/73 (BKWT) the initial tangent gave $V_{max} = 0{\cdot}75$ mmol/min and $K = 1/\overline{OB} = 0{\cdot}17$ mmol/l; the asymptote gave $\overline{OA} = 0{\cdot}33$ l/mmol, and the slope 0·82 min/l. The independently measured blood flow

was 1·46 1/min. We note first that both the undistributed and distributed models predict the slope of the asymptote to be $[F(1-\overline{OA}/\overline{OB})]^{-1}$ and hence $F = [0{\cdot}82(1-0{\cdot}056)]^{-1} = 1{\cdot}29$ 1/min. Both models therefore suggest that the directly measured total hepatic flow included a component of 0·17 1 min^{-1} or 11·6% shunted past the enzymatically active sinusoids, while only the remaining 88·4% of hepatic flow was functional in relation to enzymatic elimination expressed in the observables of the models. Adopting this interpretation, we find the functional value of $V_{max}/FK = 3{\cdot}42$. Then, with $r_B = -1n\ (\overline{OB}/\overline{OA}) = 2{\cdot}88$, equation (20) yields $\varepsilon^2 = 0{\cdot}092$ ($\varepsilon = 0{\cdot}30$). It is to be noted that the above shunt estimation depends on the narrowness but not on the symmetry of the distribution of non-zero values of v_{max}.

When the value of r is too large for $\overline{OA}$ to be distinguishable from zero in practice, the method fails. This is the case for healthy human livers eliminating galactose. For example, patient O.K. equation [(BKWT), Appendix A] had $r = 9{\cdot}75$ and $K = 0{\cdot}16$ mmol l^{-1}, so that $\overline{OA} = e^{-r}/K$ predicted by the undistributed model is less than 0·0004 1/mmol, and the prediction of the distributed model with r replaced with r_B ($\varepsilon^2 \approx 0{\cdot}02$ for O.K.) is of the same order. In fact, the difference between points A and O on the plot is found to be obscured by experimental errors in this and similar cases, for which we turn to the second method of estimating ε^2.

(2) Using the *L–B* plot of $1/V$ against $1/\hat{c}$, we obtain ε^2 from the deviation of the plot of the data from the straight line (initial tangent) predicted by the undistributed model. A rough estimate is readily available from the slope-change in equation (13), and more accurate methods of determining from the whole curve (which is analyzed in Appendix B) can be used when more data-points are available than in the present example 28/73 (experimental work in progress). The method is practicable for all values of r. The shunt correction performed for method (1) above is needed here for an additional reason, arising from the use of $\bar{c}_o$ through equation (12); if intrahepatic shunts are present, the liver vein catheter detects a mixture of $\bar{c}_o$ and of c_i arriving with the shunted flow. The reconstruction of $\bar{c}_o$ from measurements requires therefore a prior estimate of the percentage shunt.

We illustrate the method by the example of pig liver 28/73 (Fig. 3). The initial tangent of the plot is again determined by the intercepts $-1/K$ and $1/V_{max}$ given above and in BKWT; its intersection with the asymptote is given by equation (B8) of Appendix B. With the above value of $r = 3{\cdot}42$, the co-ordinates of the intersection are ($-4{\cdot}52$ 1 $mmol^{-1}$, 0·31 min $mmol^{-1}$). The values of $\hat{c}$ of the points in the graph are obtained from the measured values V, c_i (given in BKWT) by calculating $\bar{c}_o = c_i - V/F$ from equation (B1) below, using the functional value $F = 1{\cdot}29$ 1 min^{-1}. Then $\hat{c}$

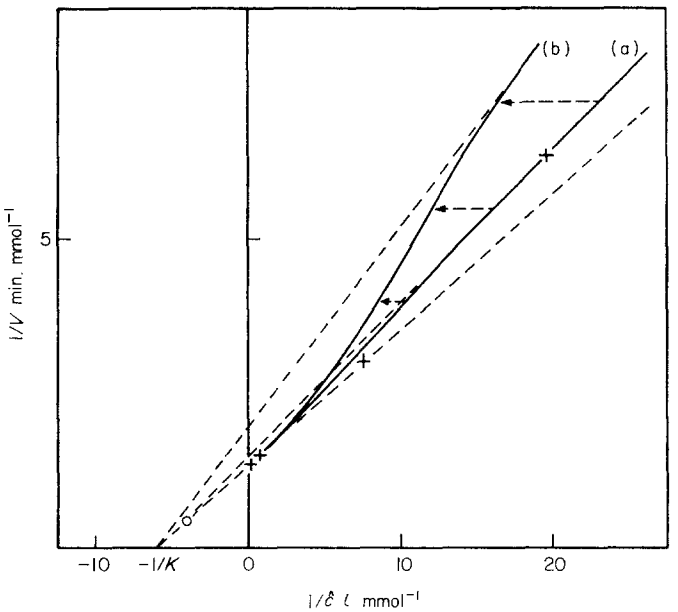

FIG. 3. Pig liver 28/73. (a) The plot of type (a) of Fig. 1. (not normalized), with experimental points ($\varepsilon^2 \approx 0{\cdot}07$), (b) Predicted transformation of plot (a) resulting from the reduction of hepatic blood flow to one third of the value in (a). The circle marks the intersection of the initial tangent with the asymptote before the flow reduction.

is calculated from equation (12) for each point. We suppose that the point at the largest $1/\hat{c}$ lies on the asymptote. The co-ordinates of that point, (19·18 1 mmol^{-1}, 6·33 min mmol^{-1}), and the intersection of the asymptote with the initial tangent, determine the asymptote. The slope of the resulting asymptote is 0·254 min 1^{-1}, while the slope of the initial tangent, $K/V_{max} = 0{\cdot}227$ is smaller by $\Delta s = 0{\cdot}027$. Hence, from equation (13), $\varepsilon^2 = 0{\cdot}07$ ($\varepsilon = 0{\cdot}264$). The agreement with the result of method (1) is fair considering the roughness of the estimates.

We illustrate also the effect of the Gaussian ε^4-correction (section 3) by the same example. With the above Δs and r used in equation (15) with $\alpha = 1/3$, ε^2 becomes 0·063.

A different class of experiments by which the distributed model may be distinguished from the undistributed one, and ε be determined, is obtained by varying the hepatic blood flow F. We note first that the value of ε of a given liver may be expected to be independent of F. This is obvious when ε is due to a distribution of v_{max}. When ε is due in part or entirely to the distribution of the flow f per sinusoid (Appendix A), ε will still not change with changes in F provided that all f's change by the same factor as F, as is

likely at least for moderate changes of flow. Such experiments yield further distinct methods of determining ε^2.

(3) Variation of $\bar{c}_o$ with F at fixed c_i. Like all effects of distributions, that variation vanishes in the homogeneous regime and increases as the clearance regime is approached. The calculated effects are complicated in the intermediate region, and the simpler and maximal effect in the clearance regime will suffice to outline the essentials. Consider equation (9): let an increment $d(1/F)$ of inverse flow bring about the increment $dr = (V_{max}/K)d(1/F)$ and hence, at fixed c_i, the relative change of $\bar{c}_o$:

$$d\bar{c}_o/\bar{c}_o = -dr(1-r\varepsilon^2). \tag{21}$$

Thus, according to the undistributed model, the relative change in $\bar{c}_o$ would be proportional to the negative increment of $1/F$, that is, $\bar{c}_o$ falls exponentially when $1/F$ is increased linearly. This powerful dependence is reduced in the distributed model by the opposing ε^2-term in equation (21) which increases in magnitude as r increases (F drops). Indications that $\bar{c}_o$ is less sensitive to changes in F at fixed c_i than predicted by the undistributed model, i.e. equation (21) with $\varepsilon^2 = 0$, have been observed (K. Winkler, pers. comm.) and will be discussed elsewhere.

(4) According to the undistributed model, equation (11) and the corresponding L–B plot are unaffected by a change in the flow F. In particular, at any fixed V (obtained experimentally by a steady infusion of substrate), a change in F should change c_i and $\bar{c}_o$ in such a way that $\hat{c}$ given by equation (12) remains unchanged. These predicted null-effects are in contrast with the following predictions from the distributed model, illustrated in Fig. 3 for pig liver 28/73 (the sketched flow-change was not actually performed).

When the flow is changed from F to F' ($F' = F/3$ in Fig. 3), the new slope-change $\Delta s'$ is again given by equation (13); hence:

$$\varepsilon^2 = 2F\Delta s = 2F'\Delta s'.$$

The change from Δs to $\Delta s'$ is brought about entirely by a swing of the asymptote, since the initial tangent pertains to the homogeneous regime and so remains unaffected by the flow. Thus the slope of the asymptote is changed by:

$$\varepsilon^2(1/F' - 1/F)/2, \tag{22}$$

from which ε^2 may be determined.

The displacement of the complete curve of the L–B plot, resulting from the change in F, follows from equation (B5) below and is illustrated in Fig. 3. At any fixed V, sufficiently high values of $\hat{c}$ are not measurably changed by flow changes, while lower values of $\hat{c}$ are increased by a reduction in F

(see arrows in Fig. 3). The former case has recently been demonstrated by Keiding and Chiarantini (1978) for the elimination of galactose by isolated perfused rat livers, the data being consistent with an ε of the order of 0·2.

We are indebted to Dr K. Winkler for permission to discuss preliminary data; to him, Professor N. Tygstrup, Dr S. Keiding, Dr J. M. Fitz-Gerald and a referee for valuable discussions; and to the Danish Medical Research Council for a grant to one of us (L.B.).

REFERENCES

AROESTY, J. & GROSS, J. F. (1970). *Microvasc. Res.* **1,** 247.
BASS, L., KEIDING, S., WINKLER, K. & TYGSTRUP, N. (1976). *J. theor. Biol.* **61,** 393.
BASS, L. & BRACKEN, A. J. (1977). *J. theor. Biol.* **67,** 637.
BASSINGTHWAIGHTE, J. B., KNOPP, T. J. & HAZELRIG, J. B. (1970). *Capillary Permeability* (C. Crone & N. A. Lassen, eds). A. Benzon Symposium II, pp. 60–80. Copenhagen: Munksgaard.
GORESKY, C. A., BACH, G. G. & NADEAU, B. E. (1973). *J. clin. Invest.* **52,** 991.
KEIDING, S., JOHANSEN, S., WINKLER, K., TØNNESEN, K. & TYGSTRUP, N. (1976). *Am. J. Physiol.* **230,** 1302.
KEIDING, S. & CHIARANTINI, E., *J. Pharmacol. Exp. Ther.* (in the press.)
POPPER, H., ELIAS, H. & PETTY, D. E. (1952). *Am. J. Clin. Path.* **22,** 717.
PRINZMETAL, M., ORNITZ, E. M., SIMKIN, B. & BERGMAN, H. C. (1948). *Amer. J. Physiol.* **152,** 48.
PROTHERO, J. & BURTON, A. C. (1961). *Biophys. J.* **1,** 565.
ROBINSON, P. Doctoral Thesis, University of Queensland, 1979.
WINKLER, K., BASS, L., KEIDING, S. & TYGSTRUP, N. (1974). *Regulation of Hepatic Metabolism* (F. Lundquist & N. Tygstrup, eds). A. Benzon Symposium VI, pp. 797–807. Copenhagen: Munksgaard.

APPENDIX A

Continuous Distributions

We now represent the distributions of v_{max}, f and v_{max}/f over the liver elements (section 1) by continuous functions. Each element is again governed by equation (1) and (2), with a common c_i for all elements.

For comparison with section 2 we develop first the case when only v_{max} is distributed. Let $\omega(v_{max})dv_{max}$ be the fraction of elements with maximum elimination rates between v_{max} and $v_{max}+dv_{max}$; $\omega(v_{max})$ is called the distribution function and its integral over all v_{max} is evidently unity. For any quantity q depending on v_{max}, the mean value $\bar{q}$ is:

$$\bar{q} = \int_0^\infty q(v_{max})\omega(v_{max})\, dv_{max}. \tag{A1}$$

Expanding $q(v_{max})$ about the mean $\bar{v}_{max}$ in a Taylor series and denoting by a

prime differentiation with respect to v_{max},

$$\left.\begin{aligned} \bar{q} &= q(\bar{v}_{max}) + \tfrac{1}{2}\sigma^2 q''(\bar{v}_{max}) + \cdots \\ \sigma^2 &= \int_0^\infty (v_{max} - \bar{v}_{max})^2 \omega(v_{max})\, dv_{max} \end{aligned}\right\}, \tag{A2}$$

where the q' term vanished by definition of the mean $\bar{v}_{max}$, and σ^2 is the variance of the distribution. In integrating term by term to obtain equation (A2), which is assumed to be a convergent or asymptotic series, we have assumed that certain conditions are satisfied by the functions q and ω. A discussion of such conditions, and the justification for assuming that they hold in the applications below, will be given elsewhere (Robinson, Ph.D. Thesis). Here we say only that we assume the distribution ω to be narrow in the following sense: for suitably smooth functions q (such as c_o, and fc_o below), the contributions to equation (A2) associated with successive moments of ω are successively smaller and such that the series converges at least asymptotically. Similar remarks apply to the distributions discussed below. Only the first two terms of the series equation (A2) will be retained in this Appendix.

We consider c_o in the role of q, its dependence on v_{max} being given implicitly by equation (1)†. Differentiating equation (1) with respect to v_{max} (with repeated use of $c_o' = -c_o f^{-1}(c_o+K)^{-1}$) we obtain $c_o'' = Kc_o f^{-2}(c_o+K)^{-3}$. Taking c_o at $\bar{v}_{max}$ and recalling the definition of the coefficient of variation, $\varepsilon = \sigma/\bar{v}_{max}$, we substitute in equation (A2):

$$\bar{c}_o = c_o(\bar{v}_{max}) + \tfrac{1}{2}\varepsilon^2 \frac{K\bar{v}_{max}^2 c_o(\bar{v}_{max})}{f^2[K + c_o(\bar{v}_{max})]^3}. \tag{A3}$$

Since the difference between $\bar{c}_o$ and $c_o(\bar{v}_{max})$ is of order ε^2, the substitution of the former for the latter in the last term of equation (A3) affects only terms of order ε^4 in the expansion in equation (A3). Writing also $\bar{v}_{max}/f = V_{max}/F$, we finally obtain:

$$\bar{c}_o = c_o(\bar{v}_{max}) + \tfrac{1}{2}\varepsilon^2 \left(\frac{V_{max}}{FK}\right)^2 \frac{K^3 \bar{c}_o}{(K+\bar{c}_o)^3}. \tag{A4}$$

We note from equation (A3) that the observable outflow concentration $\bar{c}_o$ is increased by the finite variance of the distribution as compared with the case of all v_{max} being equal to $\bar{v}_{max}$ (see discussion of equation (5), section 2). The clearance regime B is reached for $\bar{c}_o \ll K$, when equation (A4) coincides with equation (7) to order ε^2, and equation (A3) exactly.

If v_{max} is undistributed and f is narrowly distributed with some distribution function $\omega(f)$ with variance ρ^2, equation (A2) holds with f and $\bar{f}$ replacing v_{max} and $\bar{v}_{max}$, ρ^2 replacing σ^2, and with q' denoting dq/df. Because of

† Equation (A1) is then an integral equation of the first kind for the unknown function $w(v_{max})$, with the kernal c_0 given by equation (1). A mathematical treatment of this integral equation will be given elsewhere.

mixing of blood in the liver vein upstream of a catheter, the observable $\bar{c}_o$ is the *flow-weighted* mean $\overline{fc_o}/\bar{f}$, so that fc_o rather than c_o now plays the role of q in equation (A1) and (A2). Regarding fc_o a sa function of f given implicitly by equation (1), we calculate the analogue of equation (A4) according to equation (A2). The result differs from equation (A4) only in that $c_o(\bar{v}_{max})$ is replaced with $c_o(\bar{f})$, and the meaning of ε^2 becomes $\rho^2/\bar{f}^2$. We generalize these results to the cases (i) and (ii) described in the Introduction.

(i) When v_{max} and f are distributed narrowly and independently, the distribution function is factorized into the product of a function of v_{max} and a function of f. Any quantity pertaining to each element, such as fc_o, is a function of the two independent variables v_{max} and f which is given implicitly by equation (1). We expand fc_o about the point $\bar{v}_{max}, \bar{f}$ in a Taylor series in the two variables and calculate $\bar{c}_o$ by integrating term by term the double integral generalizing equation (A1), and we make use of the definitions of $\bar{v}_{max}$ and $\bar{f}$. The result differs from equation (A4) only in that $c_o(\bar{v}_{max})$ is replaced with $c_o(\bar{v}_{max}, \bar{f})$ and the meaning of ε^2 becomes:

$$\varepsilon^2 = \sigma^2/\bar{v}_{max}^2 + \rho^2/\bar{f}^2 \tag{A5}$$

which gives a concise dimensionless measure of the deviation of the liver from uniformity of elements.

(ii) When v_{max}/f is distributed narrowly and independently of a non-narrow distribution of f, the independent variables are v_{max}/f and f, and the distribution function is factorized into a product of functions of these variables. This factorization leads to the result:

$$\bar{v}_{max} = \overline{(v_{max}/f)}\bar{f}. \tag{A6}$$

Next we evaluate $\bar{c}_o$ by expanding fc_o in powers of $\overline{(v_{max}/f - v_{max}/f)}$, integrating term by term and taking advantage of the circumstance that c_o depends only on v_{max}/f according to equation (1). As a result, $\bar{c}_o$ is again analogous to equation (A4), except that $c_o(\bar{v}_{max})$ is replaced with $c_o(\overline{v_{max}/f}, \bar{f})$, and ε^2 now denotes the coefficient of variation of the distribution of v_{max}/f.

Returning to the simplest case when only v_{max} is (narrowly) distributed, we wish to eliminate the unobserved quantity $c_o(\bar{v}_{max})$. We note that equation (1) holds in particular for an element having $v_{max} = \bar{v}_{max}$ and $c_o = c_o(\bar{v}_{max})$:

$$c_i - c_o(\bar{v}_{max}) + K[\ln c_i - \ln c_o(\bar{v}_{max})] = \bar{v}_{max}/f = V_{max}/F. \tag{A7}$$

Solving equation (A4) for $c_o(\bar{v}_{max})$, substituting in equation (A7) and expanding the logarithm to order ε^2 we obtain:

$$c_i - \bar{c}_o + K \ln (c_i/\bar{c}_o) = (V_{max}/F)\left[1 - \tfrac{1}{2}\varepsilon^2 (V_{max}/FK)\frac{K^2}{(K+\bar{c}_o)^2}\right]. \tag{A8}$$

The reasoning leading to equation (A8) holds equally for all the cases considered above, except that ε^2 must be given the appropriate interpretation given above, and equation (A6) is needed in the case (ii).

APPENDIX B

The Logarithmic Average Plot

We derive and discuss the equation of the complete L–B plot of $1/V$ against $1/\hat{c}$ for the distributed model, working to order ε^2 throughout.

Averaging equation (2) over all elements we obtain $\bar{v} = \overline{fc_i} - \overline{fc_o}$. The observable $\bar{c}_o$ is the flow-weighted mean $\overline{fc_o}/\bar{f}$ (Appendix A). Using this definition and multiplying through with the number N of elements, we obtain:

$$V = F(c_i - \bar{c}_o). \tag{B1}$$

With $\ln\,(c_i/\bar{c}_o) = (c_i - \bar{c}_o)/\hat{c}$ from equation (12) and $c_i - \bar{c}_o = V/F$ from equation (B1), the left-hand side of equation (A8) becomes $(V/F)\,(1 + K/\hat{c})$. Multiplying equation (A8) through with $F/(VV_{\max})$ we obtain:

$$\frac{1}{V_{\max}}\left(1 + \frac{K}{\hat{c}}\right) = \frac{1}{V}\left[1 - \tfrac{1}{2}\varepsilon^2 (V_{\max}/FK)\,\frac{K^2}{(K + \bar{c}_o)^2}\right]. \tag{B2}$$

Next we express the $\bar{c}_o$ remaining in equation (B2) in terms of V. Since $\bar{c}_o$ occurs only in the coefficient of ε^2, we may estimate it from the undistributed model without introducing an error of order ε^2 in equation (B2). Eliminating c_i from equations (1) and (2) and writing $v_{\max}/f = V_{\max}/F$ and $v/f = V/F$ according to the undistributed model, we obtain:

$$\bar{c}_o \approx \frac{V/F}{e^{(V\max - V)/FK} - 1}. \tag{B3}$$

Setting for brevity:

$$V/FK = s, \qquad 0 < s \leqq r = V_{\max}/FK, \tag{B4}$$

we substitute equation (B3) for $\bar{c}_o$ in equation (B2) and obtain the equation of the logarithmic average plot:

$$\frac{1}{s}\left[1 - \tfrac{1}{2}\varepsilon^2\,\frac{r}{\left(1 + \dfrac{s}{e^{r-s} - 1}\right)^2}\right] = \frac{1}{r}\left(1 + \frac{K}{\hat{c}}\right). \tag{B5}$$

We consider $1/s$ as a function of $K/\hat{c}$.

The tangent at the initial point $1/s = 1/r$, $K/\hat{c} = 0$ is found to be

$$1/s = (1/r)(1 + K/\hat{c}), \tag{B6}$$

which is also obtained by setting $\varepsilon^2 = 0$ in equation (B5). The initial tangent given by equation (B6) is therefore also the full *L–B* plot for the undistributed model. The asymptote of equation (B5) at $1/s \to \infty$ is found to be:

$$\frac{1}{s}(1 - \tfrac{1}{2}r\varepsilon^2) + \frac{r\varepsilon^2}{e^r - 1} = \frac{1}{r}\left(1 + \frac{K}{\hat{c}}\right). \tag{B7}$$

We note that the slope $d(1/s)/d(K/\hat{c})$ in equation (B7) is $1/r+\varepsilon^2/2$ to order ε^2, whereas the slope in equation (B6) is $1/r$; on returning to the original variables, the difference gives the key result [equation (13)]. The intersection of the tangent (B6) with the asymptote (B7), useful in the determination of ε^2 from data (section 4), has the co-ordinates:

$$1/s = 2/(e^r-1), \quad K/\hat{c} = 2r/(e^r-1)-1. \tag{B8}$$

It can occur on either side of the $1/s$-axis ($K/\hat{c} = 0$ gives approximately $r = 1{\cdot}25$): compare cases (c) and (b) with case (a), Fig. 1.

Types of curves satisfying equation (B5) are best classified by examining the existence of an intersection of (B5) with its asymptote (B7) in the physiologically meaningful range (B4). Combining equation (B5) with equation (B7) we obtain:

$$\left(1+\frac{s}{e^{r-s}-1}\right)^{-2} = 1-\frac{2s}{e^r-1}$$

or, after some re-arrangement,

$$e^{-s} = e^{-r}\left\{1+\frac{e^r-1}{2}\left[\left(1-\frac{2s}{e^r-1}\right)^{\frac{1}{2}}+1-\frac{2s}{e^r-1}\right]\right\} \equiv g(s). \tag{B9}$$

Having denoted the right-hand side of equation (B9) by $g(s)$, we observe that (B5) and (B7) intersect in the relevant interval if and only if $g(s)$ and e^{-s} intersect there. All the features of $g(s)$ used below are readily deduced from equation (B9).

Throughout the interval $0 < s \leqslant r$, $g(s)$ and e^{-s} fall monotonically from their common point at $s = 0$ (point at infinity in terms of $1/s$); $g(s)$ is concave, e^{-s} is convex (Fig. 4). If therefore at $s = 0$ the slope of $g(s)$ is steeper (more negative) than the slope of e^{-s}, i.e.,

$$3e^{-r}/2 > 1 \quad \text{or} \quad r < 0{\cdot}405,$$

there is no intersection for positive s (case (c), Fig. 4). If the inequality of the initial slopes is reversed, an intersection exists but it may occur at an unphysiological value $s > r$ (case (a), Fig. 4). To ensure an intersection at $s < r$, we note that e^{-r} is reached by e^{-s} at $s = r$, and by $g(s)$ at $s = (e^r-1)/2$. An intersection at $s < r$ requires therefore:

$$(e^r-1)/2 < r \quad \text{or} \quad r < 1{\cdot}25.$$

Altogether, an intersection in the physiologically significant interval $0 < s \leqslant r$ occurs for r satisfying:

$$\ln(3/2) < r < 1{\cdot}25 \tag{B10}$$

(Fig. 4, case (b): compare equation (B8) *et seq.*).

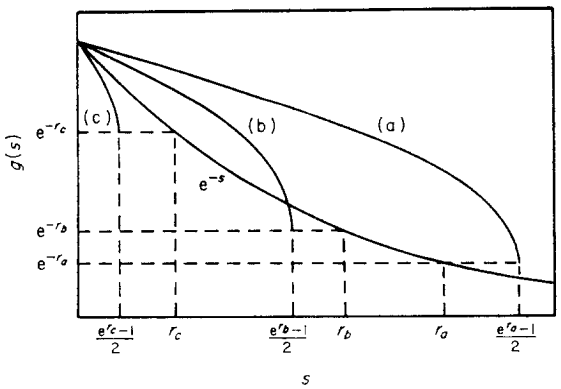

FIG. 4. Classification of the types of plots described in Fig. 1, in terms of the relation between $g(s)$ and e^{-s}. The labels (a), (b) and (c) refer to ranges of $r = V_{max}/FK$ given in Fig. 1.

Thus the main features of the plots are determined by the values of $r = V_{max}/FK$ (Fig. 1): in the case (c) the plot remains above the asymptote throughout, and there is no inflexion. The plots are s-shaped in cases (a) and (b), the former remaining below the asymptote throughout. Preliminary experiments on the elimination of galactose and ethanol by human and pig livers yielded plots of type (a) (K. Winkler, private communication of data), as expected from the values of $r > 1{\cdot}25$ in all these cases. Test substances resulting in smaller values of r are expected to yield examples of plots of types (b) and (c).

APPENDIX C

Effects of Transverse Diffusion

The ratio of the transverse equilibration time τ to the transit time T in liver sinusoids is small (less than 10^{-2}, as estimated in the Introduction) but finite. Having neglected the small quantity τ/T up to now, we consider its effects on observables c_o and V according to the undistributed model. We estimate the upper limit of the magnitude and flow-dependence of these effects and compare them with effects of distributions. We note that effects of finite equilibration time of the hepatocytes (Bass & Bracken, 1977) are similar to those of the transverse diffusion time, but more difficult to estimate for hepatocytes *in situ*.

In the steady state of the undistributed model BKWT, the longitudinal flux is Fc; the increment Fdc of that flux across two infinitesimally neighbouring sections placed at right angles to the flow at $x, x+\mathrm{d}x$, is equal to the elimination by the enzyme placed between the sections. If the enzyme density per unit length of sinusoids (each of length L) is constant, the maximum elimination rate between the sections is $V_{max}\mathrm{d}x/L$. When transverse equilibration of substrate in each cross-section is incomplete, c in the flux Fc must be interpreted as the mean concentration over the area of the cross-section, while elimination occurs at the concentration existing at the walls of the sinusoids, say $\tilde{c}$:

$$F\,\mathrm{d}c = -V_{max}(\mathrm{d}x/L)\frac{\tilde{c}}{\tilde{c}+K}, \tag{C1}$$

where $c > \tilde{c}$ and c tends to $\tilde{c}$ as τ/T tends to zero.

An estimate of the relation between c and $\tilde{c}$ is obtained by considering diffusion in a cross-section moving with the blood: in accord with the meaning of τ, c tends to the instantaneous $\tilde{c}$ with the relaxation time τ,

$$\tau\frac{\mathrm{d}c}{\mathrm{d}t} = \tilde{c}-c < 0, \tag{C2}$$

while, denoting with A the sum of cross-sections of all sinusoids,

$$\frac{\mathrm{d}x}{\mathrm{d}t} = F/A \tag{C3}$$

describes the motion. Writing $c' = \mathrm{d}c/\mathrm{d}x$, $\mathrm{d}c/\mathrm{d}t = c'(\mathrm{d}x/\mathrm{d}t)$ and using equation (C3) in (C2), we obtain:

$$\tilde{c} = c+(\tau F/A)c'. \tag{C4}$$

Recalling that $TF = AL$ and substituting from equation (C4) in (C1), we obtain:

$$Fc' = -(V_{max}/L)\frac{c+(\tau/T)Lc'}{c+(\tau/T)Lc'+K}. \tag{C5}$$

For a vanishing τ/T, the basic relation of BKWT leading to equation (1) is recovered. When τ/T is small, $K \ll c$ again yields the homogeneous regime A of section 2 independent of τ/T, while $K \gg c$ yields the clearance regime B in the form:

$$Fc' = -(V_{max}/L)\frac{c+(\tau/T_l)Lc'}{K},$$

or

$$F\left(1+\frac{V_{max}}{FK}\frac{\tau}{T}\right)c' = -(V_{max}/LK)c. \tag{C6}$$

Integrating from the inlet at $x = 0$, $c = c_i$ to the outlet at $x = L$, $c = c_o$

we obtain the counterpart of equation (4),

$$c_o = c_i \, e^{-(\tilde{V}_{max}/FK)},$$

where we have set:

$$\tilde{V}_{max} = V_{max} \Big/ \left(1 + \frac{V_{max}}{FK} \frac{\tau}{T}\right),$$

or, to first order in τ/T,

$$\tilde{V}_{max} = V_{max} \left(1 - \frac{V_{max}}{FK} \frac{\tau}{T}\right), \tag{C7}$$

Comparison of equation (C7) with equation (10) shows that in the clearance regime the modification of V_{max} by transverse diffusion is the same as that by the distributed model with $\varepsilon^2/2 = \tau/T$, in the lowest order of both effects. In particular, the slope-change Δs in the logarithmic average plot is therefore τ/FT, corresponding to the slope-change in equation (13). The full *L–B* plot resulting from the integration of equation (C5) is, of course, different from equation (B5), but it connects the limiting regimes A and B in a qualitatively similar manner.

When both ε^2 and τ/T are small but finite, they modify the undistributed model independently of each other, so that $\tilde{V}_{max}$ in equation (C7) becomes an apparent V_{max} reduced both by distributions and by incomplete transversal diffusion, which we call $\tilde{V}^B_{max}$:

$$\tilde{V}^B_{max} = V_{max} \left(1 - \frac{V_{max}}{FK} (\varepsilon^2/2 + \tau/T)\right). \tag{C8}$$

Thus the slope-change in the distributed model becomes

$$\Delta s = \frac{\varepsilon^2}{2F} + \frac{\tau}{FT}. \tag{C9}$$

We examine the main features of equation (C9) by which the two contributions to Δs can be distinguished.

(a) The diffusional upper limit of the magnitude of τ/FT may be estimated outright. For example, for galactose in liver 28/73, $\tau/FT \lessapprox 0{\cdot}01/1{\cdot}29 = 0{\cdot}0077$ min/l while $\Delta s \approx 0{\cdot}027$ min/l (section 4). In such cases the main contribution is thus due to distributions, but the detection of higher order distribution effects (section 3) may be complicated by the diffusion term, possibly enhanced by the hepatocyte equilibration time.

(b) If the term τ/FT makes an appreciable contribution to Δs, then the substitution of another substrate with a larger diffusion coefficient (shorter τ) should give a smaller Δs in the same liver at the same blood flow. In a preliminary test with both galactose and ethanol in one patient this effect was

not observed (K. Winkler, private communication), indicating that the second term in equation (C9) was small as compared with the first, in agreement with earlier results on transverse equilibration of small molecules in capillaries (Bassingthwaighte, Knopp & Hazelrig, 1970). However, substitution of another substrate with a sufficiently small diffusion coefficient may be expected to increase Δs.

(c) When blood flow is changed, $\varepsilon^2/2F$ varies linearly with $1/F$ (section 4), while τ/FT can change only in so far as the blood volume $FT = AL$ of the liver may change with the flow. The two terms in equation (C9) may therefore be separated by the study of the slope and the intercept of the plot of Δs against $1/F$ (work in progress).